Synthesis and characterization of CuS, CuS/graphene oxide nanocomposite for supercapacitor applications

Cite as: AIP Advances 10, 035307 (2020); doi: 10.1063/1.5132713
Submitted: 19 October 2019 • Accepted: 12 February 2020 •
Published Online: 4 March 2020

Rahul Singhal,[1,a)] David Thorne,[1] Peter K. LeMaire,[1] Xavier Martinez,[2] Chen Zhao,[2] Ram K. Gupta,[2] David Uhl,[3] Ellen Scanley,[3] Christine C. Broadbridge,[3] and Rakesh K. Sharma[4]

AFFILIATIONS

[1]Central Connecticut State University, New Britain, Connecticut 06050, USA
[2]Department of Chemistry, Pittsburg State University, Pittsburg, Kansas 66762, USA
[3]Connecticut State Colleges and Universities (CSCU) Center for Nanotechnology, Southern Connecticut State University, New Haven, Connecticut 06515, USA
[4]Department of Chemistry, Indian Institute of Technology Jodhpur, NH-62, Karwar, Jodhpur 342037, Rajasthan, India

[a)]**Author to whom correspondence should be addressed:** singhal@ccsu.edu. **Telephone:** +1-860-904-3723

ABSTRACT

Supercapacitors or electrochemical capacitors are receiving greater interest because of their high-power density, long life, and low maintenance. We have synthesized CuS nanoparticles and graphene oxide (CuS–GO) nanocomposites for supercapacitor applications because of their low cost and excellent electrochemical properties. The phase purity of each material was determined using powder XRD studies. The bandgap was determined by UV-visible spectrophotometric studies. Scanning electron microscope and transmission electron microscope images revealed the nano-scale morphology of the synthesized particles. All the electrochemical measurements were conducted in a standard three-electrode configuration, using a platinum wire as the counter electrode and Hg/HgO as the reference electrode. CuS and its composites with graphene oxide on nickel foam were used as working electrodes. All the electrochemical measurements were performed in 3M KOH solution. The CuS–GO nanocomposite electrode showed a specific capacitance of 250 F/g, 225 F/g, 182 F/g, 166 F/g, 161 F/g, and 158 F/g at a current density of 0.5 A/g, 1 A/g, 5 A/g, 10 A/g, 15 A/g, and 20 A/g, respectively. CuS–GO electrodes showed a specific capacitance retention of 70% after 5000 charge–discharge cycles at a current density of 5 A/g.

INTRODUCTION

Electrochemical supercapacitors are used in a variety of applications where charge has to be accepted and delivered quickly and where high-power density is required.[1–3] Supercapacitors can satisfy many modern energy needs, with applications from hybrid electric vehicles to portable electronic devices. Various transition metal oxides and transition metal sulfide materials have been explored for supercapacitor applications. The most common among these materials are MnO_2,[4] Co_3O_4,[5] WO_3[6], ZnO,[7] RuO_2,[8] and binary metal oxides such as $MnCo_2O_4$,[9] $NiMoO_4$,[10] $CoMoO_4$,[11] and $NiCo_2O_4$.[12] Transition metal oxides have limited applications in supercapacitors because of their low electrical conductivity. It has been reported that transition-metal sulfides such as CuS exhibit better electrical conductivity (10^{-3} S/cm)[13] and thermal stability than their corresponding oxides; hence, they are found to be suitable for supercapacitor applications. Copper sulfide (CuS) has been found to be promising for supercapacitor applications because of its high theoretical capacity, low cost, abundance in nature, and environmental friendliness. Venkadesh and co-workers[14] synthesized CuS materials by the solvothermal method and showed that the morphology of CuS nanostructures depends on the solvent. "Cauliflower," "microflower," and nanoparticles of a diameter of 300 nm ± 20 nm, 43 nm ± 5 nm, and 30 nm ± 3 nm, respectively, were obtained

when water, ethanol, and water/ethanol, respectively, were used as the solvent during synthesis. Raj and co-workers[15] reported that the electrochemical supercapacitor behavior of low temperature chemical bath deposition (CBD) grown 2D nanostructured CuS thin films depends on crystallinity of the electrodes. It was reported that the thin films sintered at 250 °C showed better crystallinity than as-prepared films. The sintered and as-prepared CuS thin films showed a specific capacitance of 55.55 F/g and 30 F/g, respectively, at a current density of 3 A/g.

Carbon-based materials like graphene oxides in supercapacitor electrodes contribute to charge–storage capability through the electric double layer effect, while oxides of transition metals contribute to charge–storage via oxidation–reduction reactions that transfer charge between electrolytes and electrodes. Singhal *et al.*[16] synthesized a graphene oxide (GO)/MnO_2 nanocomposite by adding $KMnO_4$ in a solution of water and ethanol (3:1), containing 10 mg of GO. They found that the capacitance of MnO_2 and MnO_2–GO electrodes was 300 F/g and 350 F/g, respectively, at a current of 0.5 A/g. Chen and co-workers[17] found that the electrochemical performance of as-prepared nanocomposites could be enhanced by the chemical interaction between graphene oxide (GO) and MnO_2. They showed that chemically synthesized GO-MnO_2 nanocomposite materials retained about 84.1% of the initial capacitance after 1000 cycles, compared to 69.0% retained by nano-MnO_2. It was also reported that MnO_2/GO nanocomposites showed a specific capacitance of 244 F/g at a current density of 0.1 A/g, with a capacity retention of approximately 94.3% after 500 cycles.[18]

The specific capacitance of CuS/graphene oxide nanocomposites was found to improve compared to bare CuS. It was reported that at a current density of 1 A/g, the specific capacitance of graphene oxide/CuS nanocomposites was 332.8 F/g, compared to 90.5 F/g for bare CuS. The excellent performance was ascribed to the "short diffusion path and large surface area of the unique hierarchical nanostructure with nanoflake building blocks for bulk accessibility of faradaic reactions."[19]

In this paper, we report the synthesis of CuS and CuS/graphene oxide (GO) nanocomposites via the hydrothermal method for high rate supercapacitor applications.

EXPERIMENTAL

Synthesis procedure

The precursor materials copper (II) acetate monohydrate [$Cu(OOCCH_3.H_2O)$, 98.0%–102%], thiourea [CH_4N_2S, 99.0%], and 1-butanol [$CH_3(CH_2)_3OH$, 99.0%] were purchased from Alfa Aesar and were used as received. Graphene oxide (Graphenea, Spain) were also used as received.

To synthesize CuS materials, an appropriate amount of copper acetate was dissolved in a water–butanol solution for 30 min. After mixing copper acetate in the water–butanol solution, thiourea was added to this solution, followed by stirring for 1 h. The final solution was then transferred into a Teflon-lined stainless-steel autoclave and heated at 180 °C for 24 h. The resulting precipitate of CuS was recovered using a centrifuge, washed with deionized (DI) water, and dried in air for 24 h. A similar procedure was followed for the synthesis of CuS–graphene oxide composites where the only change was to add 30 mg GO into the water–butanol solution prior to adding the

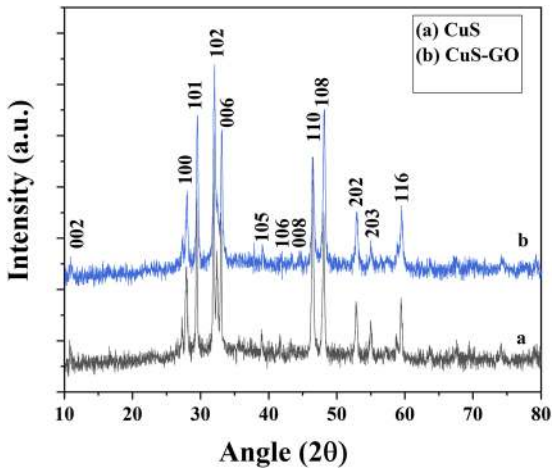

FIG. 1. X-ray diffraction pattern of CuS and CuS–GO composites.

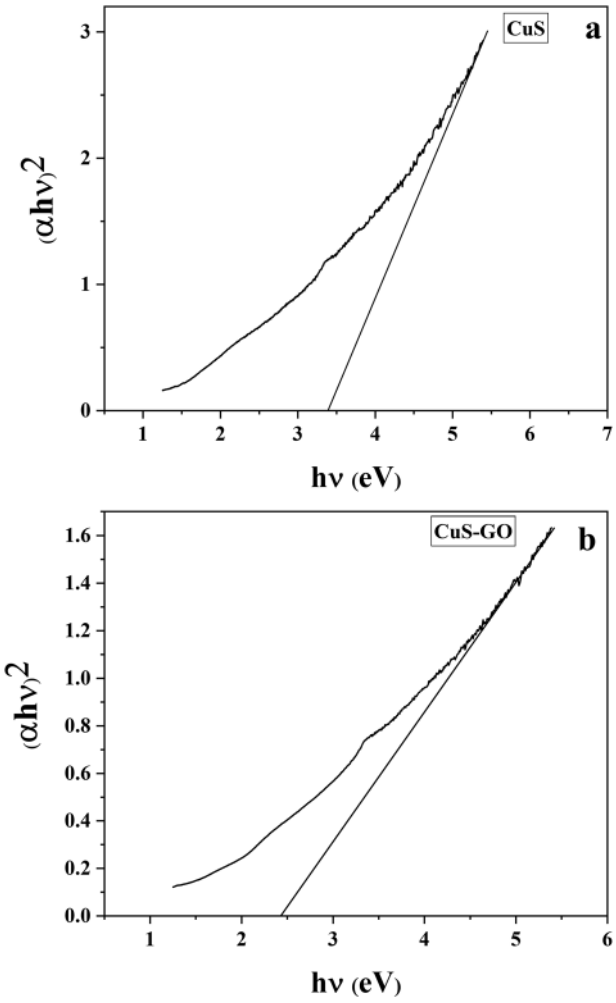

FIG. 2. Tauc plot of (a) CuS and (b) CuS–GO composites.

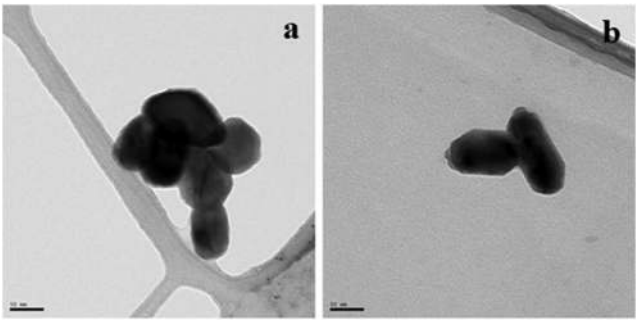

FIG. 3. TEM studies of (a) CuS and (b) CuS–GO composites.

copper acetate. The pure CuS samples and those with 30 mg GO are referred to as CuS and CuS–GO, respectively.

Characterizations

The crystal structure and phase purity of the synthesized materials were studied in an air atmosphere and at room temperature, by x-ray diffraction, using a Rigaku Mini flex-II diffractometer (CuK_α wavelength 1.5406 Å), at a scan rate of 10°/min. Data were collected at every 0.02°. The surface morphology of the synthesized materials was studied using a FEI Tecnai-12 Spirit transmission electron microscope (TEM). Images were acquired at an accelerating voltage of 120 kV. Scanning electron microscopic studies were carried out using a Hitachi tabletop scanning electron microscope (SEM, Model Hitachi TM 1000). Samples were prepared by mixing ethyl alcohol with synthesized powders, sonicating the solution, and then dipping holey-carbon TEM grids into the solution and allowing the grids to dry. Optical characterizations were carried out using a UV-visible spectrophotometer (Thermo Fisher, Evolution 220).

Working electrodes were prepared by mixing 80 wt. % of the synthesized sample, 10 wt. % of acetylene black, and 10 wt. % of polyvinylidene difluoride (PVDF) in the presence of N-methyl pyrrolidinone (NMP). After thoroughly mixing, the paste was applied onto pre-cleaned nickel electrodes, and the loading of the synthesized sample was measured by weighing the nickel foam before and after electrode preparation using an analytical balance

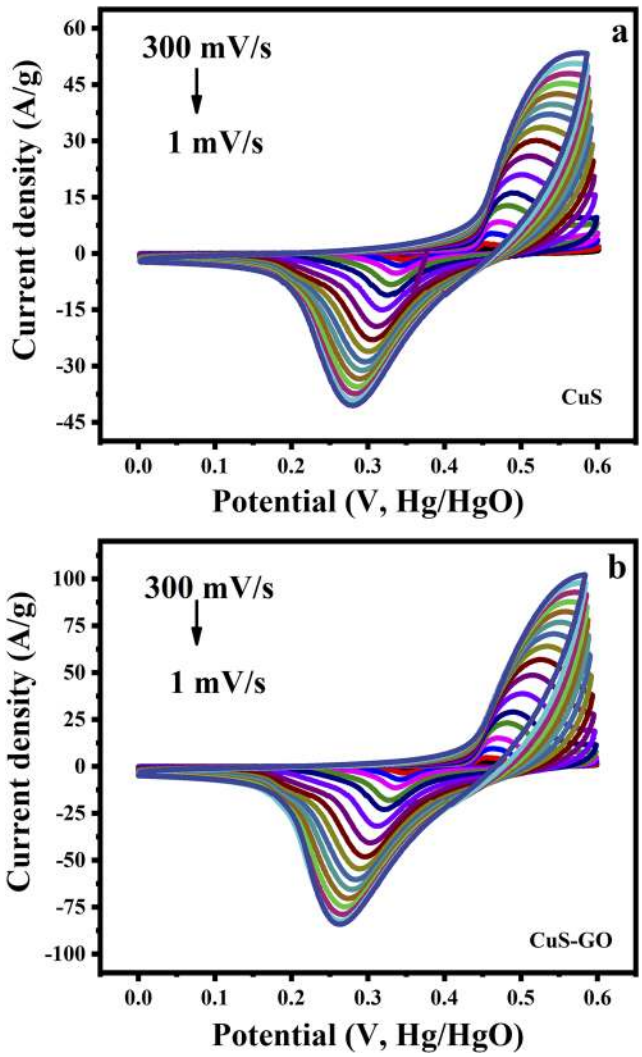

FIG. 5. Cyclic voltammogram of (a) CuS and (b) CuS–GO nanocomposite electrodes at room temperature in 3M KOH electrolyte solution as a function of scan rate.

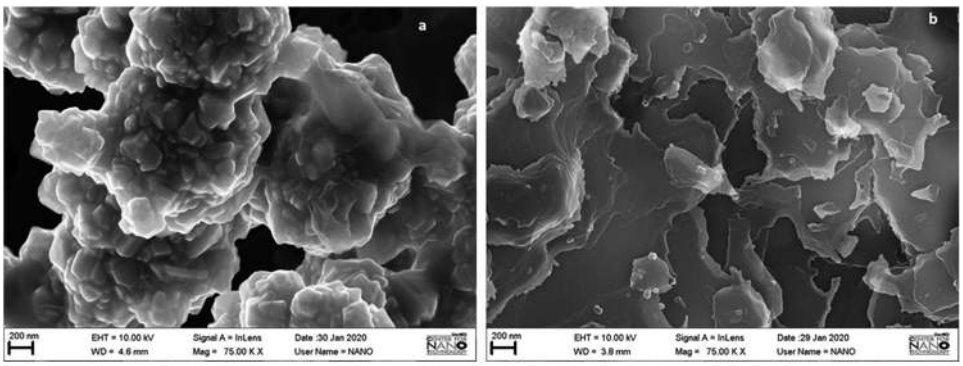

FIG. 4. SEM images of (a) CuS and (b) CuS–GO composites.

(model MS105DU, Mettler Toledo, max. 120 g, 0.01 mg of resolution). The electrochemical behavior of CuS and CuS–GO composites was studied using a VersaSTAT 4–500 electrochemical workstation (Princeton Applied Research, USA). All the electrochemical measurements were conducted in a standard three-electrode configuration, where a platinum wire and a Hg/HgO electrode was used as the counter and the reference electrode, respectively. CuS and its composites with graphene oxide on nickel foam were used as working electrodes. All the measurements were performed at room temperature in 3M KOH solution. Electrochemical properties of the synthesized samples were investigated using cyclic voltammetry (CV) and galvanostatic charge–discharge studies.

RESULTS AND DISCUSSIONS

Figure 1 shows the x-ray diffraction pattern of CuS and CuS–GO nanocomposites. The planes obtained at (100), (101), (102), (006), (110), (108), and (116) represents covellite CuS hexagonal structure. No additional peaks were found in CuS–GO composite materials as compared to CuS. These results are in agreement with those reported earlier in the literature.[15,20] The average crystallite sizes were found using the Scherrer equation,

$$D = \frac{k\lambda}{\beta \operatorname{Cos} \theta}. \quad (1)$$

Here, k is constant, λ is the CuK_α wavelength, β is the FWHM, and θ is the diffraction angle. The average crystallite size for CuS nanoparticles and CuS–GO nanocomposites were found to be about 48.3 nm and 38.1 nm, respectively.

Figure 2 shows the Tauc plots of CuS and CuS–GO nanomaterials. The bandgap energy for CuS and CuS–GO nanomaterials was found to be 3.48 eV and 2.46 eV, respectively.

Figures 3(a) and 3(b) show the TEM images of CuS and CuS–GO nanocomposites. It can be seen from the figures that all of the materials showed a hexagonal structure. The average particle size of CuS nanomaterials was found to be 95 nm and 69 nm along the long and short axis, respectively. The average particle size of CuS–GO nanocomposites was found to be 64 nm and 37 nm along the long and short axis, respectively. The results confirm that CuS–GO nanocomposites have a large surface area compared to pure CuS nanoparticles.

Figures 4(a) and 4(b) show SEM images of CuS and CuS–GO nanocomposite materials. The SEM images of bare CuS [Fig. 4(a)] show well defined nanocrystals, which agglomerate to create a microstructure. It can be seen from SEM images of CuS–GO nanocomposites that GO prevents the agglomeration of CuS nanocrystals. A similar kind of observation was earlier reported by Li and co-workers.[19]

Figures 5(a) and 5(b) show the cyclic voltammogram of CuS and CuS–GO electrodes in a potential window of 0 V–0.6 V and between scan rates of 1 mV/s to 300 mV/s. It can be seen from Figs. 5(a) and 5(b) that the oxidation and reduction peaks are clearly

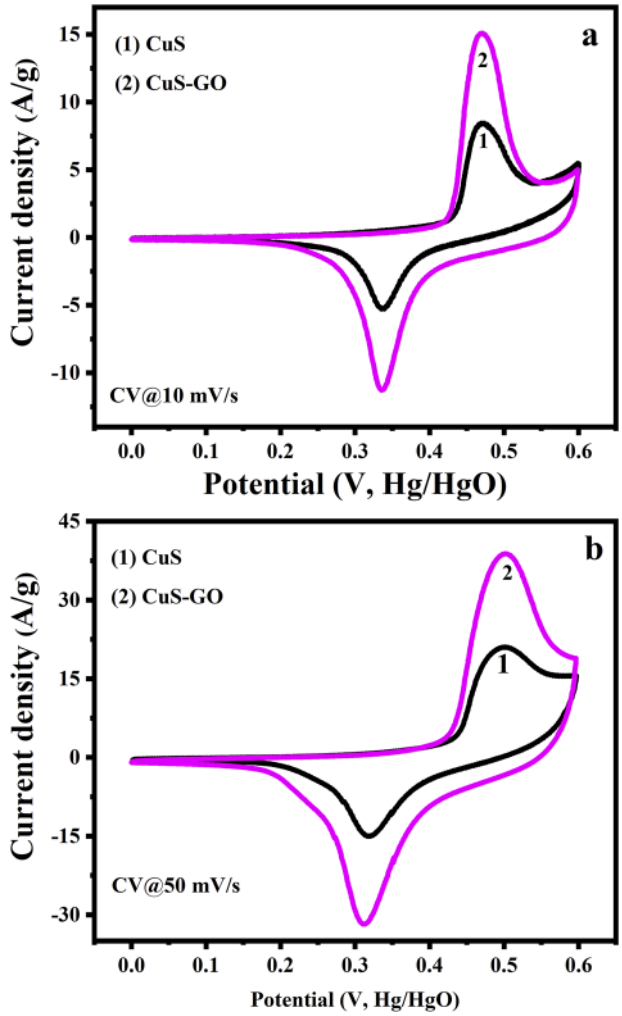

FIG. 6. Cyclic voltammogram of CuS and CuS–GO nanocomposite electrodes at a scan rate of (a) 10 mV/s (b) 50 mV/s in 3M KOH solution.

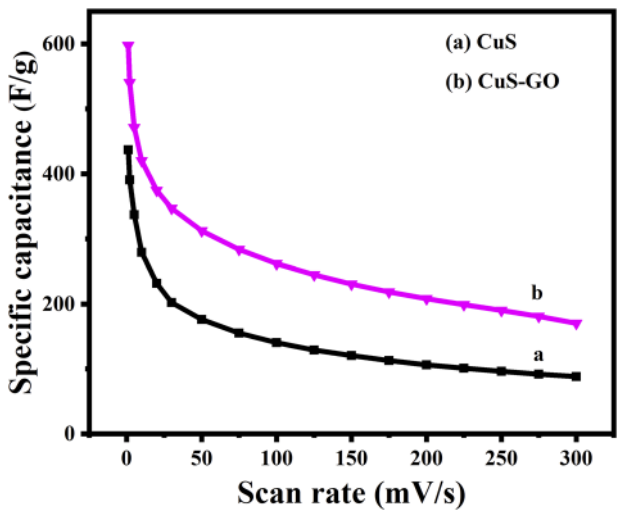

FIG. 7. Variation in specific capacitance of CuS and CuS–GO nanocomposite electrodes as a function of scan rate.

TABLE I. Specific capacitance as a function of scan rate.

	Specific capacitance (F/g)			Specific capacitance (F/g)	
Scan rate (mV/s)	CuS	CuS–GO	Scan rate (mV/s)	CuS	CuS–GO
1	437	597	125	129	262
5	337	471	150	120	230
10	279	420	175	112	218
20	231	374	200	106	208
30	202	346	225	101	198
50	176	312	250	96	190
75	155	283	275	92	181
100	140	262	300	88	170

visible, indicating that both CuS and CuS–GO show a pseudo-capacitive behavior. It can also be seen from Fig. 5 that upon increasing the scan rate, the shapes of the CV curves remain the same, indicating that the electrodes are electrochemically stable at high scan rates, that is, they have better mass transport and high rate capability.[21] Figures 6(a) and 6(b) show the cyclic voltammograms of CuS and CuS–GO nanocomposite materials at a scan rate of 5 mV/s and 10 mV/s, respectively. It can be seen from Fig. 6 that CuS–GO nanocomposites show a larger integrated area of the CV curves at both scan rates, indicating the increased charge storage capacity of CuS upon incorporation of GO in CuS. This may be because of the large surface area of GO.[22]

The specific capacitance of the synthesized samples was calculated using the following equation:

$$C_{sp} = \frac{\int I \cdot dV}{\Delta V \times \vartheta \times m}. \quad (2)$$

Here, I is the current, ΔV is the potential window, ϑ represents the scan rate, and m is the mass of the synthesized samples.

Figure 7 shows the specific capacitance of CuS and CuS–GO electrodes as a function of scan rate. It can be seen from Fig. 7 that CuS–GO nanocomposite materials showed better specific capacitance than pure CuS. The specific capacitance of CuS and

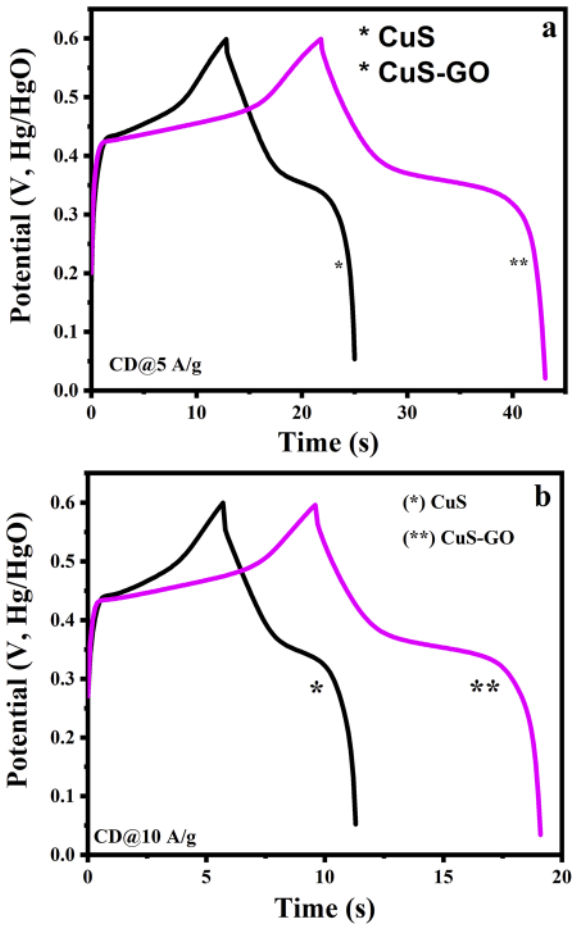

FIG. 8. Galvanostatic charge–discharge characteristics of CuS and CuS–GO nanocomposite electrodes at a current density of (a) 5 A/g and (b) 10 A/g.

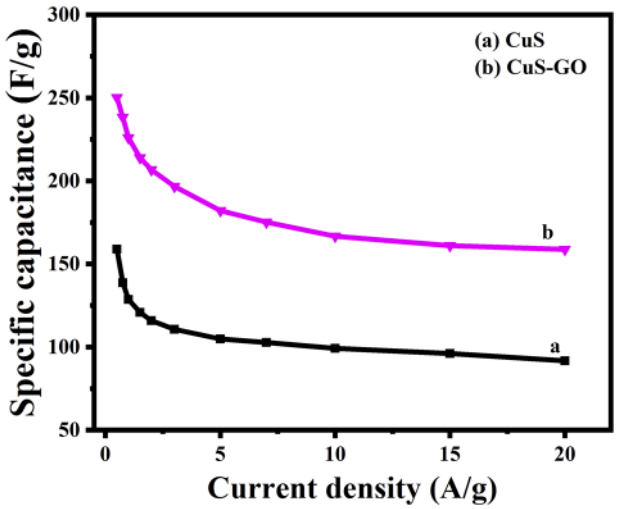

FIG. 9. Specific capacitance of CuS and CuS–GO nanocomposite electrodes as a function of current density.

TABLE II. Specific capacitance as a function of current density.

Current density (A/g)	Specific capacitance (F/g)		Current density (A/g)	Specific capacitance (F/g)	
	CuS	CuS–GO		CuS	CuS–GO
0.5	158	250	5	104	182
0.75	138	238	7	102	175
1	128	225	10	99	166
1.5	120	213	15	96	161
2	116	206	20	91	158
3	110	196	...	...	...

CuS–GO nanomaterials were found to be 437 F/g and 597 F/g, respectively, at a scan rate of 1 mV/s. Table I summarizes the specific capacitance of CuS and CuS–GO nanocomposites as a function of scan rate. It can be seen from Table I that the specific capacitance decreases gradually with increasing scan rate. This may be due to the low electrolyte ion diffusion at a high scan rate. A similar type of observation was reported by Zhao and co-workers[23] and Xu and co-workers,[20] where they reported that at a high scanning rate, ions in electrolytes cannot enter the material efficiently, so the utilization rate of the electrode material is relatively low, which results in less specific capacitance.

The specific capacitance of CuS and CuS–GO electrodes was calculated from galvanostatic charge–discharge measurements, using the following equation:

$$C_{sp} = \frac{I \times \Delta t}{\Delta V \times m}, \tag{3}$$

where I is the discharge current (A), Δt is the discharge time (s), ΔV is the potential window (V), and m is the mass (g) of the synthesized samples.

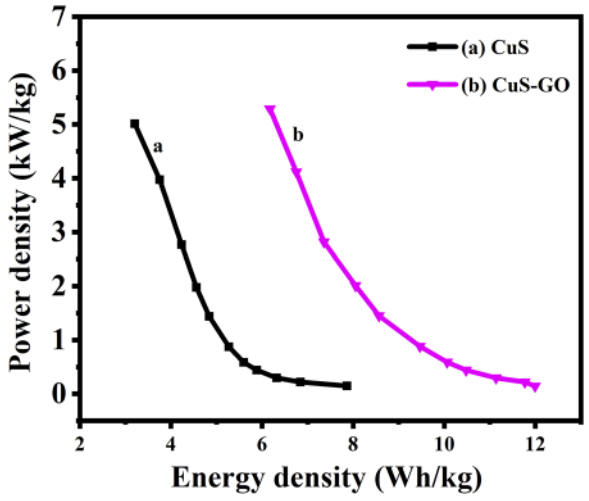

FIG. 10. Ragone plot of CuS and CuS–GO nanocomposite electrodes.

Figures 8(a) and 8(b) show the charge–discharge behavior of CuS and CuS–GO electrodes at current densities of 5 A/g and 10 A/g. It can be seen from Figs. 8(a) and 8(b) that as the current density increases, the discharge time decreases. The discharge time of CuS–GO electrodes [Fig. 8(b)] was found to be higher than that of CuS electrodes [Fig. 8(a)], indicating that the CuS–GO nanocomposite

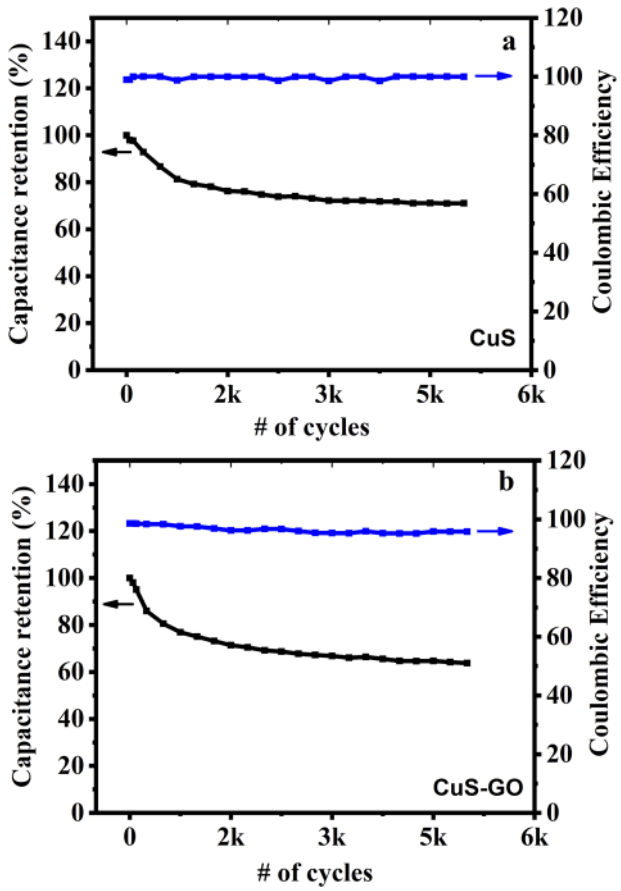

FIG. 11. Cyclic performance of (a) CuS and (b) CuS–GO nanocomposite electrodes at a current density of 5 A/g.

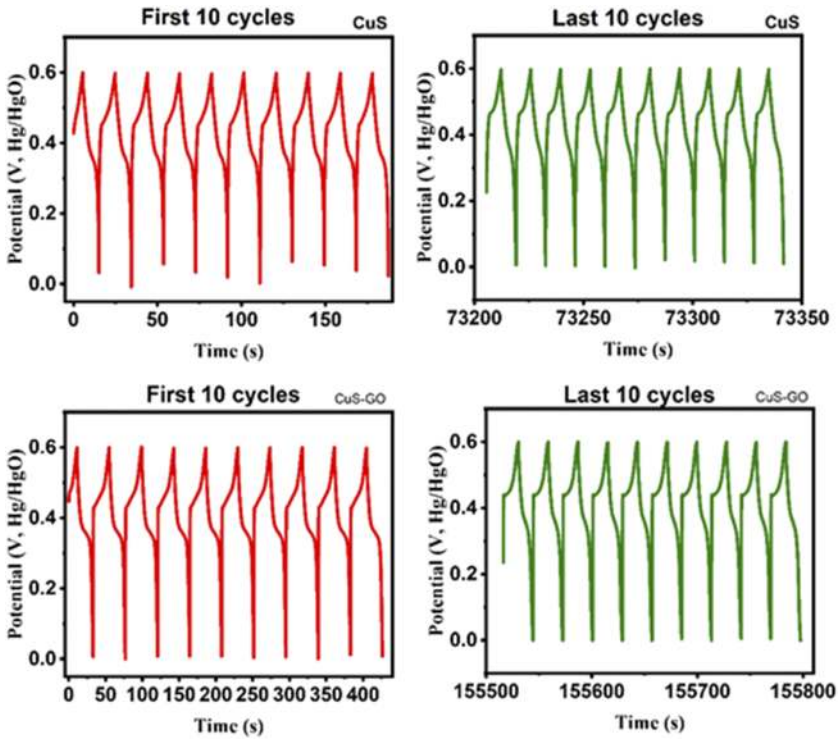

FIG. 12. Cyclic behavior of the first 10 and last 10 charge discharge cycles of CuS and CuS–GO nanocomposite electrodes at a current density of 5 A/g.

showed better specific capacitance than pure CuS. Figure 9 shows the specific capacitance of CuS and CuS–GO nanomaterials as a function of current density. The specific capacitance of CuS was found to be 158 F/g, 128 F/g, 104 F/g, 99 F/g, 96 F/g, and 91 F/g at current densities of 0.5 A/g, 1 A/g, 5 A/g, 10 A/g, 15 A/g, and 20 A/g, respectively. The specific capacitance of CuS was found to be improved in CuS–GO nanocomposites. The CuS–GO nanocomposite electrodes showed a specific capacitance of 250 F/g, 225 F/g, 182 F/g, 166 F/g, 161 F/g, and 158 F/g at a current density of 0.5 A/g, 1 A/g, 5 A/g, 10 A/g, 15 A/g, and 20 A/g, respectively. The high specific capacitance of CuS–GO nanocomposites may be due to the high surface area of GO, thus resulting in more electrolyte–electrode interactions. Table II summarizes the specific capacitance of CuS and CuS–GO nanomaterials as a function of current density. It can be seen from Table II that at a high current rate of 20 A/g, CuS electrodes show 58% of the specific capacitance shown at 0.5 A/g. On the other hand, at 20 A/g, CuS–GO nanocomposite electrodes show 63% of the specific capacitance shown at 0.5 A/g. Furthermore, the lower value of specific capacitance at high current densities than its value at a low current density can be attributed to the low ion diffusion rate at higher current densities.

Electrochemical performance of supercapacitors can be evaluated by studying energy density and power density. The energy density (W, Wh kg^{-1}) and power density (P, W kg^{-1}) can be calculated using the following equations:

$$W = C_{sp}\Delta V^2/2, \quad (4)$$

$$P = W/\Delta t, \quad (5)$$

where Δt (s) is the discharge time.

It can be seen from the Ragone plots of CuS and CuS–GO electrodes (Fig. 10) that CuS electrodes show a maximum power density of 5.0 kW/kg at an energy density of 3.2 Wh/kg and CuS–GO electrodes show a maximum power density of 5.3 kW/kg at an energy density of 6.2 Wh/kg. These results support CuS and CuS–GO as promising materials for energy storage applications.

Electrochemical stability is an important factor for use of supercapacitors in practical applications. Figure 11 shows the cyclic behavior of the first 5000 cycles of CuS and CuS–GO electrodes at a scan rate of 5 A/g. It can be seen from Fig. 11 that CuS electrodes have approximately 80% capacity retention after 5000 charge–discharge cycles, while CuS–GO electrodes show 70% capacity retention after 5000 charge–discharge cycles. Furthermore, Fig. 12 shows the characteristic of the first 10 and last 10 charge discharge cycles of CuS and CuS–GO electrodes at a current density of 5 A/g. It can be seen from Fig. 12 that both the electrodes reach up to 0.6 V even after 5000 charge–discharge cycles, which indicates that electrodes are stable upon cycling even at a high current rate of 5 A/g.

CONCLUSIONS

We have successfully synthesized CuS and CuS–GO nanocomposites. The x-ray diffraction pattern confirms the phase purity of the synthesized nanocomposites. TEM studies confirm that CuS and CuS–GO composites are nanosized. The specific capacitance of CuS–GO nanocomposites was found to increase compared to that of pure CuS. The specific capacitance of CuS and CuS–GO nanocomposites were found to be 158 F/g and 250 F/g, respectively, at a current density of 0.5 A/g. The CuS–GO nanocomposite electrodes

show a specific capacitance of 158 F/g at a current density of 20 A/g. Specific capacitance retention was studied at a current density of 5 A/g for 5000 cycles and was found to be 80% and 70% for CuS and CuS–GO nanocomposites, respectively. These results confirm that CuS and CuS–GO nanocomposites can be used for supercapacitor applications.

ACKNOWLEDGMENTS

The financial support received from the CCSU-AAUP Minority Retention and Recruitment Committee (MRRC) grant and the CCSU-AAUP Faculty Research grant is highly acknowledged. Dr. Ram K. Gupta expresses his sincere acknowledgment to the Polymer Chemistry Program and Kansas Polymer Research Center, Pittsburg State University, for providing financial and research support. We also acknowledge the use of facilities and the support from personnel from the CT State Colleges and Universities Center for Nanotechnology and the Werth Family Industry Academic Fellowship Program.

REFERENCES

[1] C. Tang, Z. Pu, Q. Liu, A. M. Asiri, X. Sun, Y. Luo, and Y. He, ChemElectroChem **2**(12), 1903–1907 (2015).
[2] Z. Xing, Q. Chu, X. Ren, C. Ge, A. H. Qusti, A. M. Asiri, A. O. A. Youbi, and X. Sun, J. Power Sources **245**, 463–467 (2014).
[3] B. Hu, X. Qin, A. M. Asiri, K. A. Alamry, A. O. A. Youbi, and X. Sun, Electrochim. Acta **107**, 339–342 (2013).
[4] J. Roberts and R. C. T. Slade, Electrochim. Acta **55**, 7460–7469 (2010).
[5] Y. Duan, T. Hu, L. Yang, J. Gao, S. Guo, M. Hou, and X. Ye, J. Alloys Compd. **771**, 156–161 (2019).
[6] P. A. Shinde, A. C. Lokhande, A. M. Patil, and C. D. Lokhande, J. Alloys Compd. **770**, 1130–1137 (2019).
[7] L. Fang, B. Zhang, W. Li, J. Zhang, K. Huang, and Q. Zhang, Electrochim. Acta **148**, 164–169 (2014).
[8] H. Xia, Y. S. Meng, G. Yuan, C. Cui, and L. Lu, Electrochem. Solid-State Lett. **15**(4), A60–A63 (2012).
[9] K. R. Shrestha, S. Kandula, N. H. Kim, and J. H. Lee, J. Alloys Compd. **771**, 810–820 (2019).
[10] X. Lu, W. Jia, H. Chai, J. Hu, S. Wang, and Y. Cao, J. Colloid Interface Sci. **534**, 322–331 (2019).
[11] S. Wen, K. Qin, P. Liu, N. Zhao, L. Ma, C. Shi, and E. Liu, Appl. Surf. Sci. **465**, 389–396 (2019).
[12] H. Gao, Y. Cao, Y. Chen, Z. Liu, M. Guo, S. Ding, J. Tu, and J. Qi, Appl. Surf. Sci. **465**, 929–936 (2019).
[13] K. J. Huang, J. Z. Zhang, and K. Xing, Electrochim. Acta **149**, 28–33 (2014).
[14] A. Venkadesh, S. Radhakrishnan, and J. Mathiyarasu, Electrochim. Acta **246**, 544–552 (2017).
[15] C. J. Raj, B. C. Kim, W. J. Cho, W. G. Lee, Y. Seo, and K. H. Yu, J. Alloys Compd. **586**, 191–196 (2014).
[16] R. Singhal, J. Fagnoni, D. Thorne, P. K. LeMaire, X. Martinez, C. Zhao, R. K. Gupta, D. Uhl, E. Scanley, C. C. Broadbridge, and M. Manivannan, MRS Adv. **4**, 777 (2019).
[17] S. Chen, J. Zhu, X. Wu, Q. Han, and X. Wang, ACS Nano **4**(5), 2822–2830 (2010).
[18] Z. Chen, J. Li, Y. Chen, Y. Zhang, G. Xu, J. Yang, and Y. Feng, Particuology **15**, 27–33 (2014).
[19] X. Li, K. Zhou, J. Zhou, J. Shen, and M. Ye, J. Mater. Sci. Technol. **34**(23), 2342–2349 (2018).
[20] W. Xu, Y. Liang, Y. Su, S. Zhu, Z. Cui, X. Yang, A. Inoue, Q. Wei, and C. Liang, Electrochim. Acta **211**, 891–899 (2016).
[21] H. Heydari, S. E. Moosavifard, M. Shahraki, and S. Elyasi, J. Energy Chem. **26**(4), 762–767 (2017).
[22] K. J. Huang, J. Z. Zhang, Y. L. Jia, K. Xing, and Y. M. Liu, J. Alloys Compd. **641**, 119–126 (2015).
[23] T. Zhao, W. Yang, X. Zhao, X. Peng, J. Hu, C. Tang, and T. Li, Composites, Part B **150**, 60–67 (2018).